

Cite this: *Soft Matter*, 2012, **8**, 4171

www.rsc.org/softmatter

PAPER

Time temperature superposition in soft glassy materials

Rahul Gupta, Bharat Baldewa and Yogesh M. Joshi*

Received 31st October 2011, Accepted 12th December 2011

DOI: 10.1039/c2sm07071e

Soft glassy materials are out of thermodynamic equilibrium and show a time dependent slowing down of the relaxation dynamics. Under such situations these materials follow a Boltzmann superposition principle only in the effective time domain, wherein time dependent relaxation processes are scaled by a constant relaxation time. In this work we extend the effective time framework to successfully demonstrate a time–temperature superposition of creep and stress relaxation data of a model soft glassy system comprised of a clay suspension. Such a superposition is possible when the average relaxation time of the material changes with time and temperature without affecting the shape of the spectrum. We show that variation in relaxation time as a function of temperature facilitates the prediction of a long and short time rheological behavior through the time–temperature superposition from the experiments carried out over experimentally accessible timescales.

I. Introduction

Very high viscosity soft materials such as concentrated suspensions and emulsions, colloidal gels, foams and pastes do not reach thermodynamic equilibrium over practical timescales due to structural arrest.^{1–3} However the natural tendency of materials to explore phase space in order to progressively attain lower potential energy state causes evolution of structure and viscoelastic properties as a function of time.^{4–7} Rheologically these materials typically demonstrate yield stress and thixotropic behavior.^{8–10} Time dependency associated with these materials, however, does not allow them to obey the most fundamental linear viscoelastic theorem, the Boltzmann superposition principle in its conventional form.¹¹ Consequently a very powerful rheological tool, time–temperature superposition, is also not applicable to this class of materials. Inapplicability of these basic linear viscoelastic principles restricts the rheological modeling capacity of these industrially important soft materials. Recently our group employed an effective time framework, originally due to Hoffman,¹² and successfully demonstrated the application of a Boltzmann superposition principle in the effective time domain to a variety of soft glassy materials.^{13,14} In this paper we extend the effective time framework to propose a procedure to carry out a time–temperature superposition in soft glassy materials.

In the limit of linear response, according to the Boltzmann superposition principle, the relaxation modulus (and equivalently creep compliance) depends only on time elapsed since the application of a deformation field.^{15,16} However, for materials that undergo time evolution of rheological properties, the relaxation modulus and creep compliance show an additional dependence on time at which the deformation field is applied.¹¹

Under such a situation, it is customary to employ an effective time approach, wherein real time with time dependent relaxation time is transformed to an effective time domain where relaxation time is constant.^{11,17} The effective time scale ξ is defined as: $\xi(t) = \int_0^t \tau_0 dt' / \tau(t')$.^{11,14,18} Since in an effective time domain relaxation time remains constant, which we consider to be an arbitrary constant τ_0 , the Boltzmann superposition principle can be restated by replacing time elapsed since application of deformation field by the effective time elapsed since the application of a deformation field. Therefore, in an effective time domain the modified Boltzmann superposition principle can be expressed as:^{11,14,18}

$$\begin{aligned} \sigma(t) &= \int_{-\infty}^t G(\xi(t) - \xi(t_w)) \frac{d\gamma}{dt_w} dt_w \quad \text{or} \\ \gamma(t) &= \int_{-\infty}^t J(\xi(t) - \xi(t_w)) \frac{d\sigma}{dt_w} dt_w, \end{aligned} \quad (1)$$

where t is present time, t_w is the time at which deformation was applied, G is the relaxation modulus, J is the creep compliance, γ is strain and σ is stress. Typically for glassy materials relaxation time is observed to show a power law dependence on time $\tau = A\tau_m^{1-\mu}t^\mu$, where τ_m is the microscopic relaxation time and A is constant.^{14,17,18} Therefore the effective time elapsed since the application of a deformation field is given by:

$$\xi(t) - \xi(t_w) = \int_{t_w}^t \tau_0 dt' / \tau(t') = \frac{\tau_0 \tau_m^{\mu-1}}{A} \left[\frac{t^{1-\mu} - t_w^{1-\mu}}{1-\mu} \right]. \quad (2)$$

Usually rheological behavior of any real material is dictated by a distribution of relaxation times. According to the definition of the effective time scale, every relaxation mode will lead to a different effective time scale. However, if the deformation field

Department of Chemical Engineering, Indian Institute of Technology Kanpur, Kanpur, 208016, India. E-mail: joshi@iitk.ac.in

does not affect the shape of the relaxation time distribution, eqn (1) can still be used to describe the viscoelastic behavior of soft glassy materials as recently described by Baldewa and Joshi.¹³

In the literature the effective time approach was first applied to glassy materials (amorphous polymers) by Struik.¹⁷ However, unlike the treatment of effective time discussed in the present paper, Struik considered only the limit of $t - t_w \ll t_w$ (process time much smaller than aging time) in order to neglect aging during the process time. In this limit eqn (2) leads to: $\xi(t) - \xi(t_w) = [\tau_0 \tau_m^{\mu-1} (t - t_w)] / [A t_w^\mu]$ (Struik used a different procedure to get a similar result in the limit: $t - t_w \ll t_w$. For convenience we have derived this expression directly from eqn (2)). This limiting expression suggests that creep compliance or relaxation modulus will demonstrate a time–aging time superposition, if process time ($t - t_w$) is normalized by that factor of relaxation time which depends on aging time (t_w^μ). Many researchers demonstrated the validity of the time–aging time superposition in the limit of $t - t_w \ll t_w$ (also known as Struik protocol) for amorphous polymers,^{17,19} spin glasses^{20,21} and soft glassy materials.^{22–26} In order to avoid errors induced in the analysis because of the approximation of eqn (2) and consideration of the narrow range of process time, the time–aging time superposition was attempted directly in the effective time domain and in recent years its application was successfully demonstrated for a variety of soft glassy materials.^{13,14,27,28}

Observation of the superposition in the effective time domain also leads to the prediction of long time behavior of creep compliance or relaxation modulus.^{13,14} Prediction of a long time behavior from time–aging time superposition is aided by a change in relaxation time at different aging times. Similar to aging time, the deformation field and temperature also influence the relaxation time and its dependence on aging time. Recently Baldewa and Joshi studied effect of the deformation field and observed that it induces nonlinear effects thereby affecting the distribution of relaxation times.¹³ Awasthi and Joshi²⁴ studied the effect of temperature on aging and also proposed a time–temperature superposition for creep flow of a Laponite suspension using the Struik protocol. However, the previous methodology was strongly limited by the predictive capability.²⁴ In this work we study the superposition behavior of creep compliance and relaxation modulus in an effective time domain at different temperatures. We demonstrate a time–temperature superposition in an effective time domain and show that it leads to greater predictive capacity of long and short time rheological behavior.

II. Materials and experimental procedure

In this work we use 2.8 weight % aqueous suspension of Laponite RD,[®] which is known to demonstrate various characteristic features of soft glassy behavior.²⁹ Laponite RD consists of disk shaped particles having diameters around 30 nm and thicknesses of 1 nm and was procured from Southern Clay Products Inc.³⁰ Dry Laponite powder was mixed with ultrapure water having pH 10 using an Ultra Turrex drive for a period of 30 min. Subsequently the suspension was stored for a predetermined period in sealed polypropylene bottles. The detailed preparation protocol to prepare aqueous suspension of Laponite is discussed elsewhere.³¹

In this work we carry out creep and step strain experiments using an Anton Paar MCR 501 rheometer (Couette geometry,

bob diameter 5 mm and gap 0.2 mm). We carry out these experiments at 5 different temperatures in the range 15–55 °C. For creep experiments we use an 80 day old Laponite suspension while for the step strain experiments we use a 54 day old Laponite suspension. It is important to note that due to irreversible aging demonstrated by Laponite suspension over a duration of days, 80 day and 54 day old Laponite suspension should be considered as different systems altogether.³¹ For creep experiments a new sample is used in each experiment, while in the case of the step strain experiments the same sample was used for all the experiments carried out at a given temperature. At the beginning of each experiment, after the thermal equilibrium was reached, the sample was shear melted by applying an oscillatory flow field having a strain magnitude of 1500 at a frequency of 0.1 Hz for 15 min. Shear melting is necessary to obtain the same initial conditions in all the experiments and therefore usage of the same sample or a new sample does not make any difference. Subsequent to shear melting, the sample was allowed to age. The corresponding evolution of elastic modulus during aging was probed by applying small amplitude oscillatory shear with strain magnitude 0.5% at a frequency 0.1 Hz. After carrying out aging for a predetermined period of time, a constant shear stress (5 Pa) or step strain (3%) was applied to the suspension. In order to avoid drying and contamination of CO₂, the free surface of suspension was covered with a thin layer of low viscosity silicone oil.

III. Results and discussion

In Fig. 1 the evolution of elastic modulus is plotted as a function of aging time. It can be seen that the evolution of elastic modulus shifts to lower aging times for experiments carried out at higher temperatures. Aging in soft glassy materials is usually accompanied by the enhancement of a characteristic relaxation time as well as the modulus as a function of waiting time. If we consider a caged entity in a glassy material to have a barrier height associated with an energy well to be E , then relaxation time can be considered to have an Arrhenius dependence on E given by: $\tau = \tau_m \exp(E/k_B T)$.¹¹ Typically, from scaling analysis the elastic modulus can be represented as energy density and can be expressed as: $G' = E/b^3$,³² where b is the characteristic length-scale associated with the glassy material. Therefore enhancement of relaxation time and modulus with time suggests a state of the

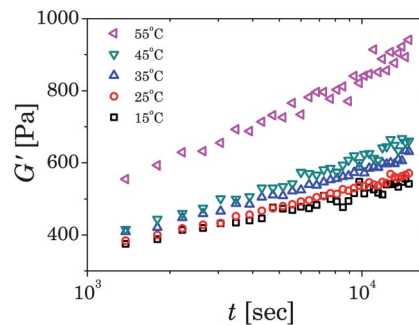


Fig. 1 Evolution of elastic modulus as a function of time for 54 day old aqueous Laponite suspension. Evolution shifts to lower times for experiments carried out at higher temperatures.

system with greater barrier height of the energy well (or a lower potential energy state). A shift in the evolution of G' to low aging times at higher temperatures therefore suggests a decrease in microscopic time (timescale associated with microscopic rearrangement) at which the system explores the phase space and lowers its energy. The evolution of elastic modulus as a function of aging time then can be represented by: $G' = G_0 \ln(t_w/\tau_m)$, which can be considered to have an Arrhenius dependence on temperature (and therefore becomes fast at higher temperatures). Enhanced aging at higher temperatures appears to be a characteristic feature of many glassy materials such as molecular glasses,³³ and various soft glassy materials.^{34–37}

Subsequent to the aging step, we performed creep experiments on 80 day old aqueous Laponite suspension samples. The corresponding evolution of creep compliance for experiments carried out at different aging times is plotted in the inset of Fig. 2a. It can be seen that compliance induced in the material decreases for the experiments carried out at higher aging times. We also carry out step strain experiments on 54 day old Laponite suspensions. The stress relaxation subsequent to step strain, plotted in the inset of Fig. 2b, shows slower relaxation for experiments carried out at higher aging times. The insets in Fig. 2a and 2b therefore demonstrate that compliance as well as stress relaxation modulus do not depend solely on time elapsed since the application of a deformation field but also show an additional dependence on time at which deformation was applied. This behavior is not in agreement with the Boltzmann

superposition principle. However, as suggested before, the Boltzmann superposition principle can be applied to such a class of materials in an effective time domain, wherein it is proposed that compliance is the sole function of effective time elapsed since the application of a deformation field. In Fig. 2a and 2b we plot vertically shifted compliance and relaxation modulus respectively, as a function of $[t^{1-\mu} - t_w^{1-\mu}]/(1-\mu)$, wherein we assume power law dependence of relaxation time on aging time ($\tau = A\tau_m^{1-\mu}t_w^\mu$). It can be seen that compliance and stress relaxation modulus data show an excellent superposition in the effective time domain for a certain value of μ . The observed time–aging time superposition also leads to the validation of the Boltzmann superposition principle in the effective time domain. Importantly the fitted value of μ suggests a rate of enhancement of relaxation time as a function of aging time: $\mu = d \ln \tau / d \ln t_w$.

We perform creep and stress relaxation experiments at different aging times over a range of temperatures. In Fig. 3a and 3b, we plot time–aging time superpositions for creep compliance and relaxation modulus obtained at various temperatures. Due to enhanced elastic modulus and viscosity, compliance induced in the material is lower for experiments carried out at higher temperatures. Equivalently, relaxation of stress is slower for experiments performed at higher temperatures. In Fig. 4, we plot the value of μ , needed to obtain the time–aging time superposition, as a function of the reciprocal of temperature. Over a range of temperatures studied in this work, μ can be seen to be following a linear dependence on $1/T$. If we assume two expressions of relaxation times: $\tau = A\tau_m^{1-\mu}t_w^\mu$ and $\tau = \tau_m \exp(E/k_B T)$, to be equivalent and substitute two relations for elastic modulus: $G' = G_0 \ln(t_w/\tau_m)$ and $G' = E/b^3$, we get: $\mu \propto G_0 b^3 / k_B T$ (actually

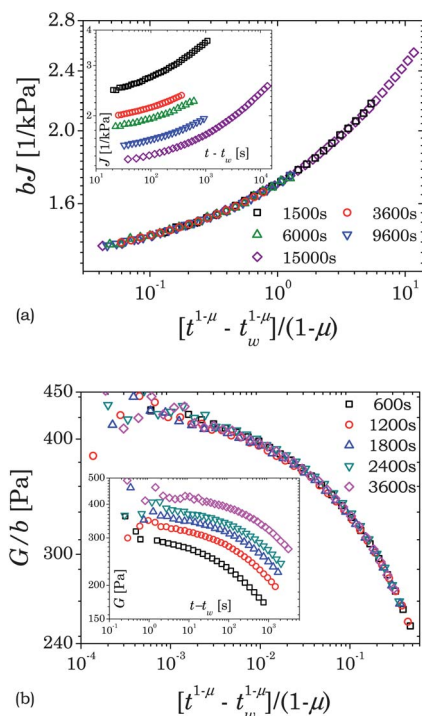


Fig. 2 Time–aging time superposition for creep compliance (a), and for stress relaxation modulus (b) in the effective time domain. The insets in respective figures show evolution of (a) compliance (55 °C) and (b) stress relaxation modulus (25 °C) as a function of time. The vertical shift factor is given by $b = G(t_w)/G(t_w, R)$ in the limit $t - t_w \rightarrow 0$. $G(t_w, R)$ is the modulus at the reference aging time (t_w, R).

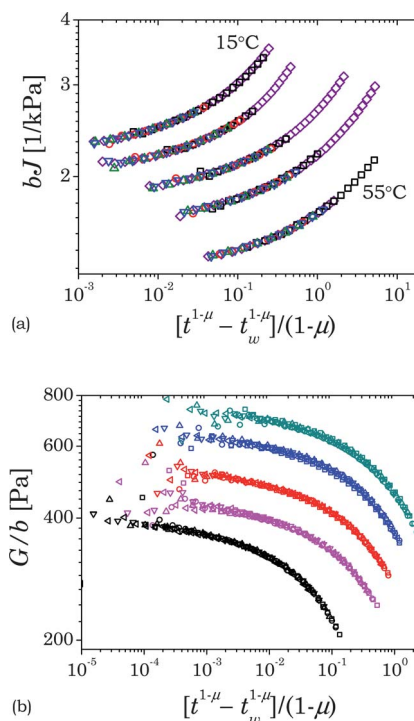


Fig. 3 Time–aging time superpositions at different temperatures. (a) For creep experiments, from top to bottom: 15, 25, 35, 45, 55 °C. (b) For stress relaxation experiments, from top to bottom: 55, 45, 35, 25, 15 °C.

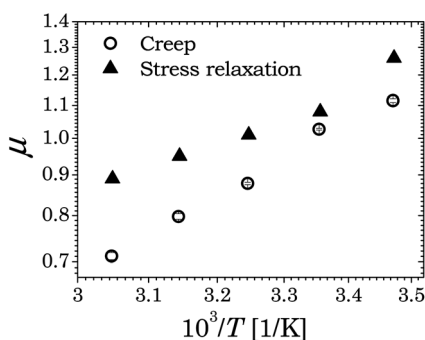


Fig. 4 Dependence of factor μ on temperature.

$\mu = [G_0 b^3 / k_B T] - [G_0 b^3 \ln A / E]$, however the very fact that μ remains constant with respect to the aging time suggests that the second term is negligible compared to the first term, $E \gg k_B T \ln A$). Interestingly, the experimental observation shown in Fig. 4 is in qualitative agreement with this dependence.

It can be seen that the time–aging time superpositions obtained at different temperatures described in Fig. 3a and 3b have self-similar curvatures. By carrying out horizontal and vertical shifting we obtain a comprehensive time–aging time–temperature superposition for creep compliance (Fig. 5a) and stress relaxation modulus (Fig. 5b). It should be noted that in the superposition of creep data we have considered the data obtained at 55 °C and $t_w = 15\,000$ s only up to 1500 s of creep time. The motivation behind the consideration of partial data is to enable

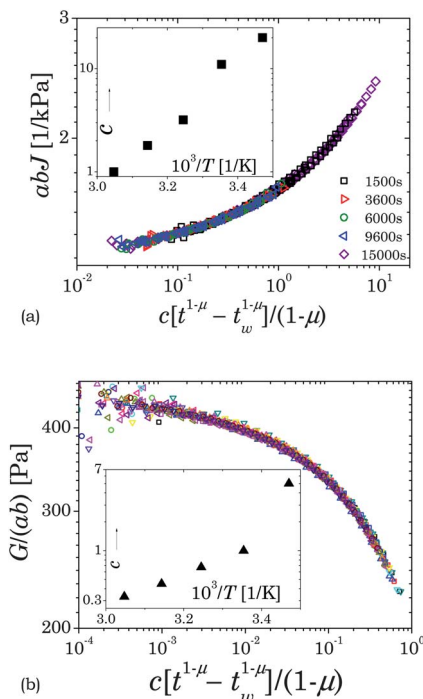


Fig. 5 Time–aging time–temperature superposition in an effective time domain for (a) creep experiments, and (b) step strain experiments. The insets in respective figures show dependence of horizontal shift factor on temperature. Vertical shift factor is given by $a = G(t_w, T) / G(t_w, T_R)$ in the limit $t - t_w \rightarrow 0$. We consider reference temperature (T_R) to be 55 °C for creep while 25 °C for step strain experiments.

the prediction of the remaining data as discussed below. A vertical shift factor is necessary to compensate for the enhancement in an elastic modulus as a function of temperature at a given aging time. On the other hand, a horizontal shift factor is necessary to accommodate changes in relaxation time as a function of temperature. It should be noted that in an effective time domain the rheological data should be represented as a function of $[\xi(t) - \xi(t_w)] / \tau_0$ for every temperature. However for convenience, in Fig. 2 and 3, we divide the difference in effective time by $\tau_0 \tau_m^{\mu-1} / A$ leading to: $\{[\xi(t) - \xi(t_w)] / (\tau_0 \tau_m^{\mu-1} / A) = (t^{1-\mu} - t_w^{1-\mu}) / (1 - \mu)\}$. Consequently in order to represent the abscissa of Fig. 5 as $[\xi(t) - \xi(t_w)] / \tau_0$ a horizontal shift factor should scale as $c \propto \tau_m^{\mu-1} / A$. In order to shift individual superpositions on to a superposition at a reference temperature, the horizontal shift factor should therefore scale as: $c = \tau_m^{\mu-1} / \tau_m^{\mu R} = \tau_m^{\mu-1} / \tau_m^{\mu R}$. As discussed before, if we assume microscopic time to have an Arrhenius dependence on temperature $\tau_m = \tau_{m0} \exp(\bar{U} / k_B T)$, where τ_{m0} is an attempt time while \bar{U} is energy barrier associated with microscopic movement of the entity within the cage, we get: $\ln c \propto \frac{G_0 b^3}{k_B T} \left(\ln(\tau_{m0}) + \frac{\bar{U}}{k_B T} \right)$ (\bar{U} should not be confused with E , which is the barrier height associated with the energy well). As shown in the insets of Fig. 5a and 5b, the observed linear dependence of $\ln c$ on reciprocal of temperature suggests an increase in the relaxation time as a function of temperature.

Time–aging time–temperature superpositions shown in Fig. 5a and 5b suggest that the material will follow the evolution of creep compliance or stress relaxation modulus in an effective time domain as per superposition, if experiments were carried out at respective reference temperatures. Since at reference temperature, $c = 1$, superpositions described in Fig. 5a and 5b can be transformed back into real time domains as suggested by Shahin and Joshi.¹⁴ If we consider the abscissa of Fig. 5 to be $\theta = [t^{1-\mu} - t_w^{1-\mu}] / (1 - \mu)$, the real time elapsed since the application of a deformation field can simply be represented by:

$$t - t_w = \{\theta(1 - \mu) + t_w^{1-\mu}\}^{1/(1-\mu)} - t_w. \quad (3)$$

As shown in Fig. 5, the superposition extends beyond the original creep or stress relaxation data available at the reference temperature and aging time. Therefore, transformation of the superposition from an effective time domain to the real time domain leads to prediction of a long time as well as a short time behavior. In Fig. 6a and 6b, we plot creep and stress relaxation time data at reference temperature and aging times, and compare the same with a corresponding prediction by transforming the superposition using eqn (3). For the creep data associated with 55 °C and $t_w = 15\,000$ s, data that were not considered in the superposition (1500 to 15 000 s) are represented by down triangles. It can be seen that the proposed procedure predicts the overall creep data very well. The benefit of time–aging time–temperature superposition described in Fig. 5 over time–aging time superposition plotted in Fig. 2 can be appreciated better from the superposition associated with stress relaxation data wherein we consider complete data in the superposition. The information available from Fig. 3b is over the range of θ from 5×10^{-4} to 0.45 while the same from Fig. 5b is available in the range 2×10^{-4} to 0.8, which according to eqn (3) will lead to a prediction over broader creep times. The procedure also leads to the prediction of very short time rheological behavior as well.

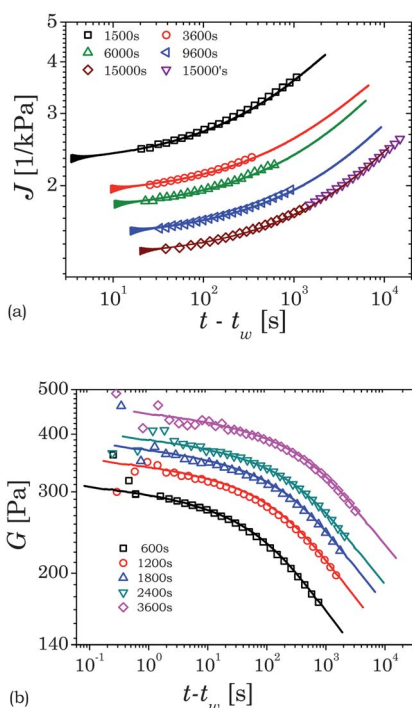


Fig. 6 Prediction of the long and short time rheological behavior (a) creep experiments (55 °C), and (b) stress relaxation experiments (25 °C). Symbols are experimental data while lines are the predictions.

We feel that prediction of short time behavior is also very important as very small time regimes are usually not accessible due to instrument inertia and data acquisition speeds.

It is important to note that the fundamental basis of the time–temperature superposition described in Fig. 5 and that carried out in equilibrated soft materials such as polymeric liquids is identical. In the later systems relaxation time of the material decreases with an increase in temperature and therefore experiments carried out at higher temperatures facilitate the description of long time creep or stress relaxation behaviors.¹⁵ For the present system, closer inspection of Fig. 3 and 5 indicates that superpositions obtained at low temperatures facilitate the prediction of long time rheological behavior of experiments carried out at higher temperatures. Conversely, the superposition corresponding to high temperatures leads to a description of very short time rheological behavior. This observation suggests that at low temperatures the aqueous suspension of Laponite has a smaller relaxation time at a given aging time. Interestingly, Fig. 4 indicates that μ , which describes logarithmic dependence of relaxation time on aging time ($d \ln \tau / d \ln t_w$), decreases with an increase in temperature. Considering both these aspects, in Fig. 7 we schematically describe dependence of relaxation time on aging time as a function of temperature. Fig. 7 suggests that, although greater in magnitude, the relaxation time at higher temperatures evolves slowly.

In order to observe the time–temperature superposition for equilibrium soft materials, the shape of the relaxation time distribution needs to remain unaffected by a change in temperature. The same is also true for soft glassy materials.¹³ Therefore, in order to observe the time–aging time–temperature superposition, the shape of the relaxation time distribution needs to be

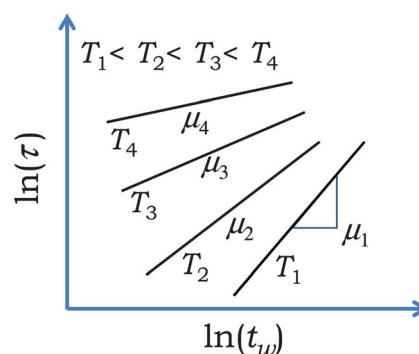


Fig. 7 Schematic describing the dependence of a characteristic relaxation time on aging time as a function of temperature.

unaffected by variations of aging time as well as temperature. Similar curvatures of rheological data reported in the insets of Fig. 2 and that of superpositions shown in Fig. 3 essentially suggest that the shape of the distribution has remained unaffected by aging time and temperature respectively. We believe that this is the only constraint which needs to be fulfilled for the observation of time–temperature superposition for any soft glassy material in the effective time domain. The specific details of how relaxation time and modulus behave as a function of temperature may be material specific and will only affect the predictive capacity of the superposition. We hope that the time–temperature superposition procedure developed in this work for soft glassy materials will be tested for a variety of non-ergodic systems and will prove helpful in characterizing these industrially important complex fluids.

IV. Conclusions

Soft glassy materials exhibit temporal evolution of their structure and viscoelastic properties. Particularly the relaxation dynamics of soft glassy materials is observed to become sluggish with respect to time. Consequently compliance or modulus exhibits an additional dependence on time at which the deformation field was applied disregarding the Boltzmann superposition principle in its conventional form. Transformation of the rheological data to effective time domain, wherein all the relaxation processes are rescaled by considering a constant relaxation time, allows the application of the Boltzmann superposition principle. The compliance or stress relaxation modulus is observed to demonstrate time–aging time superposition when plotted in the effective time domain irrespective of time of application of deformation field. In this work we extend the effective time framework to demonstrate time–temperature superposition in creep as well as step strain (stress relaxation) experiments. We employ aqueous Laponite suspension as a model soft glassy material. In this system we observe that the relaxation time of the material is greater while it's temporal evolution in logarithmic scale ($d \ln \tau / d \ln t_w$) is weaker at higher temperatures. The time–aging time superpositions obtained at different temperatures show similar curvature in the effective time domain, thereby enabling the time–aging time–temperature superposition by horizontally shifting the data. Self-similar curvatures of the creep data suggest that temperature affects only the average value of relaxation time and not the shape of the distribution, which in turn is a criterion

for observing the time–temperature superposition. Owing to the enhanced relaxation time with increase in temperature, experiments carried out over accessible timescales at lower temperatures facilitates prediction of long time behavior at higher temperatures through time–temperature superposition. Similarly prediction of short time data is aided by experiments performed at higher temperatures.

Acknowledgements

This work was supported by Department of Science and Technology, Government of India under IRHPA scheme.

References

- 1 L. Cipelletti and L. Ramos, *J. Phys.: Condens. Matter*, 2005, **17**, R253–R285.
- 2 P. Coussot, *Lect. Notes Phys.*, 2006, **688**, 69–90.
- 3 M. E. Cates and M. R. Evans, *Soft and fragile matter*, The institute of physics publishing, London, 2000.
- 4 G. B. McKenna, T. Narita and F. Lequeux, *J. Rheol.*, 2009, **53**, 489–516.
- 5 S. A. Rogers, P. T. Callaghan, G. Petekidis and D. Vlassopoulos, *J. Rheol.*, 2010, **54**, 133–158.
- 6 D. J. Wales, *Energy Landscapes*, Cambridge University Press, Cambridge, 2003.
- 7 C. Christopoulou, G. Petekidis, B. Erwin, M. Cloitre and D. Vlassopoulos, *Philos. Trans. R. Soc. London, Ser. A*, 2009, **367**, 5051–5071.
- 8 N. Koumakis and G. Petekidis, *Soft Matter*, 2011, **7**, 2456–2470.
- 9 P. Coussot, *Rheometry of Pastes, Suspensions and Granular Materials-Application in Industry and Environment*, Wiley, Hoboken, 2005.
- 10 J. Mewis and N. J. Wagner, *Advances in Colloid and Interface Science*, **147–148**, pp. 214–227.
- 11 S. M. Fielding, P. Sollich and M. E. Cates, *J. Rheol.*, 2000, **44**, 323–369.
- 12 I. L. Hopkins, *J. Polym. Sci.*, 1958, **28**, 631–633.
- 13 B. Baldewa and Y. M. Joshi, *Soft Matter*, 2012, **8**, 789–796.
- 14 A. Shahin and Y. M. Joshi, *Phys. Rev. Lett.*, 2011, **106**, 038302.
- 15 R. B. Bird, R. C. Armstrong and O. Hassager, *Dynamics of Polymeric Liquids, Fluid Mechanics*, Wiley-Interscience, New York, 1987.
- 16 H. A. Barnes, J. F. Hutton and K. Walters, *An Introduction to Rheology*, Elsevier, Amsterdam, 1989.
- 17 L. C. E. Struik, *Physical Aging in Amorphous Polymers and Other Materials*, Elsevier, Houston, 1978.
- 18 S. M. Fielding, Ph.D. Thesis, University of Edinburgh, 2000.
- 19 P. A. O’Connell and G. B. McKenna, *Polym. Eng. Sci.*, 1997, **37**, 1485–1495.
- 20 G. F. Rodriguez, G. G. Kenning and R. Orbach, *Phys. Rev. Lett.*, 2003, **91**, 037203.
- 21 P. Sibani and G. G. Kenning, *Phys. Rev. E: Stat., Nonlinear, Soft Matter Phys.*, 2010, **81**, 011108.
- 22 M. Cloitre, R. Borrega and L. Leibler, *Phys. Rev. Lett.*, 2000, **85**, 4819–4822.
- 23 P. Coussot, H. Tabuteau, X. Chateau, L. Tocquer and G. Ovarlez, *J. Rheol.*, 2006, **50**, 975–994.
- 24 V. Awasthi and Y. M. Joshi, *Soft Matter*, 2009, **5**, 4991–4996.
- 25 Y. M. Joshi and G. R. K. Reddy, *Phys. Rev. E: Stat., Nonlinear, Soft Matter Phys.*, 2008, **77**, 021501–021504.
- 26 A. Shaukat, A. Sharma and Y. M. Joshi, *Rheol. Acta*, 2010, **49**, 1093–1101.
- 27 C. Derec, G. Ducouret, A. Ajdari and F. Lequeux, *Phys. Rev. E: Stat. Phys., Plasmas, Fluids, Relat. Interdiscip. Top.*, 2003, **67**, 061403.
- 28 B. Baldewa and Y. M. Joshi, *Polymer Engineering and Science*, 2011, **51**, 2084–2091.
- 29 D. Bonn, S. Tanasc, B. Abou, H. Tanaka and J. Meunier, *Phys. Rev. Lett.*, 2002, **89**, 157011–157014.
- 30 <http://www.laponite.com>.
- 31 A. Shahin and Y. M. Joshi, *Langmuir*, 2010, **26**, 4219–4225.
- 32 R. A. L. Jones, *Soft Condensed Matter*, Oxford University Press, Oxford, 2002.
- 33 A. J. Kovacs, *J. Polym. Sci.*, 1958, **30**, 131–147.
- 34 G. Ovarlez and P. Coussot, *Phys. Rev. E: Stat., Nonlinear, Soft Matter Phys.*, 2007, **76**, 011406.
- 35 P. Agarwal, H. Qi and L. A. Archer, *Nano Lett.*, 2009, **10**, 111–115.
- 36 X. Di, K. Z. Win, G. B. McKenna, T. Narita, F. Lequeux, S. R. Pallela and Z. Cheng, *Phys. Rev. Lett.*, 2011, **106**, 095701.
- 37 P. Agarwal, S. Srivastava and L. A. Archer, *Phys. Rev. Lett.*, 2011, **107**, 268302.